Closed-Path *J*-Integral Analysis of Bridged and Phase-Field Cracks

Roberto Ballarini
Department of Civil and Environmental Engineering,
University of Houston,
Houston, TX 77004
e-mail: rballarini@uh.edu

Gianni Royer-Carfagni
Department of Industrial Engineering,
University of Parma,
Parma 43124, Italy
e-mail: gianni.royer@unipt.it

We extend the classical J-integral approach to calculate the energy release rate of cracks by prolonging the contour path of integration across a traction-transmitting interphase that accounts for various phenomena occurring within the gap region defined by the nominal crack surfaces. Illustrative examples show how the closed contours, together with a proper definition of the energy momentum tensor, account for the energy dissipation associated with material separation. For cracks surfaces subjected to cohesive forces, the procedure directly establishes an energetic balance à la Griffith. For cracks modeled as phase-fields, for which no neat material separation occurs, integration of a generalized energy momentum (GEM) tensor along the closed contour path that traverses the damaged material permits the calculation of the energy release rate and the residual elasticity of the completely damaged material. [DOI: 10.1115/1.4032986]

Keywords: fracture, cohesive fracture, phase-field model, J*-integral, Eshelby tensor, energy release rate, small-scale bridging limit*

1 Introduction

In his fundamental paper of 1951, Eshelby [1] opened new possibilities in the physical theory of the solid state by showing a parallelism with the classical theory of elasticity. Specifically, he demonstrated that the driving force for the movement of a source of elastic singularity such as a point defect within a crystal lattice can be established as the negative gradient of the total energy with respect to the position of the singular point. In his words, "this force, in a sense fictitious, is introduced to give a picturesque description of energy changes, and must not be confused with the ordinary and surface and body forces acting on the material." The distinction is emphasized by defining the driving forces as *configurational forces* which are associated with a balance law for a tensorial field referred to as the *energy–momentum tensor*. More precisely, at the base of the energy release rate associated with the movement of the singularity, there is a configurational force balance that must hold for any arbitrary control volume of the body. Although initially considered for linear elastic materials, the energy–momentum tensor and the corresponding balance laws can be defined for nonlinear elastic solids [2] and, for processes where dissipative phenomena are involved, for which a variational derivation is not straightforward. Gurtin recognized the broad and deep significance of configurational forces by viewing them as basic primitive objects, consistent with their own force balance [3].

In this paper, we address cracks that involve dissipative phenomena, and therefore, it is useful to refer to Gurtin's derivation of the Eshelby relation that does not involve any constitutive equation or variational principle but instead relies upon a version of the second law for referential control volumes whose boundaries evolve with time. For the sake of simplicity, we summarize the procedure for the case of infinitesimal deformation gradients (small stains and moderate rotation); extension to nonlinear deformations does not present additional conceptual difficulties but only a slightly larger mathematical effort. Then, let $\Omega \subset \mathrm{R}^d$, where d is the dimension where the problem is set, be representative of the undistorted reference configuration of the body, and let $\mathbf{u}(\mathbf{x})$: $\Omega \rightarrow \mathrm{R}^d$ represent the displacement of a particle initially at $\mathbf{x} \in \Omega$. Following the same argument of Ref. [4], if one assumes the energy–momentum tensor $\mathbf{T}$ as a primitive quantity for which an appropriate form of the second law of thermodynamics is introduced, one can demonstrate that invariance under reparameterization of the reference control volume provides the Eshelby relation

$$\mathbf{T} = \Psi \mathbf{I} - \nabla \mathbf{u}^T \mathbf{S} \tag{1.1}$$

where Ψ is the bulk free energy of the body, $\mathbf{I}$ is the identity tensor, $\mathbf{S}$ is the deformational stress tensor, and $\delta\mathbf{u}$ is the displacement gradient. The tensor $\mathbf{T}$ has proven to be useful in the formulation of numerous physical problems, such as evolving interfaces, two-phase equilibrium, and solidification processes. In particular, for the motion of a line in a two-dimensional body [5], the significant balance law is of the type

$$\int_\Gamma (\Psi - \nabla \mathbf{u}^T \mathbf{S})\mathbf{n}\, ds + \mathbf{g} = \mathbf{0} \tag{1.2}$$

where $\mathbf{g}$ is the concentrated configurational force associated with its tip, and Γ is an *arbitrary* closed surface that embraces the tip. If the direction of the moving line is defined by the unit vector $\mathbf{r}$, one readily has

$$-\mathbf{g}\cdot\mathbf{r} = \mathbf{r}\cdot\int_\Gamma (\Psi - \nabla \mathbf{u}^T \mathbf{S})\mathbf{n}\, ds = \int_\Gamma (\Psi \mathbf{r}\cdot\mathbf{n} - \mathbf{S}\mathbf{n}\cdot\nabla\mathbf{u}\mathbf{r})\, ds \tag{1.3}$$

This relationship is the basis of the elegant method proposed by Rice [6] to calculate the energy release rate of a crack. The procedure is well defined because the integral in Eq. (1.3), traditionally referred to as the *J*-integral, is path independent as long as the area enclosed by the closed path does not include singularities.

When calculating the *J*-integral for topological features such as a line, the path Γ can *embrace* the tip of the line and *touch* the crack surfaces, rendering Γ a *closed* contour. But if the line represents a crack whose surfaces introduce a discontinuity of

Contributed by the Applied Mechanics Division of ASME for publication in the Journal of Applied Mechanics. Manuscript received February 26, 2016; final manuscript received March 9, 2016; published online March 29, 2016. Editor: Yonggang Huang.

displacements, then it acts as a barrier that cannot be trespassed and thus prevents Γ from closing. Whether the path Γ should be considered closed or not is a subtle but substantial distinction. Consider the case of a line (or surface) of discontinuity for which the displacement field is multivalued. In the case of infinitesimal deformations, the (infinitesimal) strain-tensor field cannot be integrated in a cut body even if it satisfies the compatibility equations because, using, for example, Cesaro's representation [7], one would obviously reach different values of the displacement while approaching the two faces of the cut from opposite sides. In general, multivalued displacements are encountered when the reference domain Ω is not periphractic,[1] which for the two-dimensional case coincides with the notion of multiply connected. A similar difficulty occurs when the body is continuous but obtained from a configuration that is not periphractic in the natural undistorted state, for example, Volterra dislocations for which material portions are first added or subtracted and then the cutting surfaces are joined together. As suggested by Love [8], a physical interpretation of the mathematical problem may consist in rendering the domain periphractic by means of a system of barriers, isolating the two faces of any discontinuity surface. The stress in the body is one valued and continuous, but the displacement may be discontinuous across the barrier.

Similarly to the aforementioned example, the energy momentum tensor $\mathbf{T}$, even if it is divergence free, may provide a nonzero value when integrated on a closed contour Γ embracing a crack tip. It is then useful, in the definition of Γ, to imagine that the slits present in the body are associated with topological barriers, in the sense mentioned above, and that Γ touches the two faces of the barrier, but does not traverse it. This setting is used in the classical application of the *J*-integral, as suggested by Rice [6].

The situation is different for cracks whose surfaces are subjected to tractions, such as those introduced by Barenblatt [9]. In the most general case, the surfaces of such cracks are subjected to cohesive forces *per* unit area that are functions of the crack opening displacement (COD). If one regards such forces as being provided by a fictitious interphase layer of infinitesimal but non-null thickness, then the displacement at the interface is no longer multivalued, because the image point of each particle forming the interphase is well defined. Therefore, for cohesive cracks there is no need to introduce a topological barrier along the line defining the crack, and as a consequence, a completely closed path that enters and traverses the interphase material may be considered. This idea is presented in Sec. 2.1 with reference to a paradigmatic example.

The cohesive interphase, referred to as the process zone, allows for material separation at the price of energy dissipation, because the constitutive relationship that relates the cohesive forces *per* unit area to the COD presents a strain softening branch approaching the null value at a critical value of the COD. This contribution enters the global energetic balance of the system and, according to Griffith's basic idea, the crack advances when the energy release rate equals the rate of dissipation of the cohesive forces in the process zone. Therefore, modulo a proper definition of the energy–momentum tensor, one expects that the vanishing of the *J*-integral on a Γ that traverses the interphase, according to Eq. (1.3), represents the condition of crack extension. This direct approach for establishing Griffith equilibrium is illustrated in Sec. 2.2.

The idea of closing the path of the *J*-integral is directly applied to the case of a Barenblatt crack under monotonic loading in Sec. 3.2, under the assumption that the crack profile remains self-similar as it extends, as discussed in Sec. 3.1. It is noted that the same argument for such smooth closure cracks can be applied in the small-scale bridging limit to establish a correlation with the borderline case of sharp cracks. In this case, the evanescent interphase zone triggers and produces the neat separation of the material ligaments, a process that should be recalled in the energetic balance by considering that material separation is associated with the cohesive law. Consequently, one can repeat the same rationale used for cohesive forces and take into account directly the contribution *à la* Griffith for the energy dissipated in the fracturing process. In this case, the stress intensity factor is not zero, but it can be directly verified that the closed-path *J*-integral, traversing the crack in the sense mentioned above, vanishes.

The closed-path *J*-integral approach described in this paper is analogous to Eshelby's approach for bodies containing defects like dislocations, where there is no barrier and the integral of the energy momentum tensor is always performed on a closed contour. Remarkably, this approach can naturally be extended to the case of bridged cracks in linear elastic materials, for which the cohesive forces are not sufficient to annihilate the crack tip stress intensity factor. As shown in Sec. 3.3, this can be done *via* an appropriate definition of the generalized energy–momentum tensor, slightly different from Eq. (1.2): integration of this field along a *closed* path embracing the crack tip can directly provide the energy release rate associated with the square of the stress intensity factor at the crack tip.

The closed-path *J*-integral method can readily be applied to phase-field models of crack propagation. In classical models of fracture, cracks are well-defined lines or surfaces of discontinuity. In the phase-field approach, on the contrary, cracks are viewed as narrow bands in which the material degrades. Many recent works aim at establishing a link between these two somewhat complementary views of the same phenomenon. Various forms of phase-field models have been proposed, for which an excellent review can be found in Ref. [10]. For the sake of illustration, in Sec. 4.1 reference will be made to the models by Karma et al. [11], later developed by Hakim and Karma [12] and by Bourdin et al. [13]. In particular, the latter authors used modern results of variational convergence of functionals [14] to connect, in the limit of the evanescent length-scale l associated with the fracture geometry, a rate-independent damage theory of the gradient type [15] to the variational approach to brittle fracture [16]. A key parameter in the aforementioned limit $l \to 0$ is the assumption that a positive quantity, infinitesimal faster than l, is added to the elastic part of the strain energy in the corresponding functional. In the approximating phase-field model, such a quantity must be considered in order to stabilize the numerical solution of the minimization problem, but not too much consideration is paid to this, because the aforementioned convergence result suggests that it is small and negligible. Nevertheless, such quantity produces a residual nonzero stiffness (of the order of a small fraction of the elastic modulus as determined through numerical results) in the damage bands, producing an effect that, for the case of sharp cracks, would be equivalent to bridging forces along crack surfaces.

A detailed analysis of the possible use of the *J*-integral in the phase-field description of cracked bodies has been conducted by Hakim and Karma [12]. The authors first introduced the generalized energymomentum (GEM) tensor, which contains a term that accounts for the damaging phase field. The configurational forces exerted on a propagating damage band can thus be obtained by considering the flux of the GEM tensor on the "open" path *ACB*, of the type represented in Fig. 1. Here, *A* and *B* are taken sufficiently far from the tip and close to the crack on a macroscopic scale, but with the distance $2h$ between *A* and *B* much longer than the process zone scale. Namely, the mathematical limits $h \to +\infty$ and $R \to +\infty$, with $h/R \to 0$, are followed, where *R* is the distance of *A* and *B* from the crack tip. This represents, for the case of phase-field models, the counterpart of the topological barrier mentioned above for the case of sharp cracks. Since on the path *ACB*, the material is sound, the GEM tensor reduces to the classical

[1]A three-dimensional cracked body is not "periphractic" in a topological sense general, according to the definition of Milne-Thomson. He noted its Greek derivative meaning "fenced about" and characterized a periphractic three-dimensional region as one that is "bounded internally by one or more closed surfaces." Thus, a periphractic three-dimensional region has embedded holes or cracks, but not necessarily holes that pierce completely through it. The former is simply connected but the latter is not.

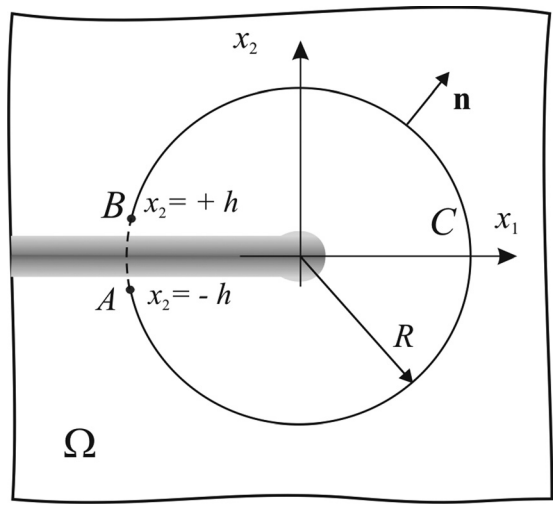

Fig. 1 Spatially diffused crack tip region. Circular contour path to calculate the flux of the GEM tensor.

Eshelby tensor, so that one obtains the energy release rate with an argument that mirror's Rice's *J*-integral.

It is noted that some ambiguities arise in the aforementioned procedure. The phase field does not present a sharp transition from 0 (broken material) to 1 (sound material), so that the exact width of the process zone cannot be defined in objective terms. One could certainly define the region where the field is $1-\phi_0$, with $\phi_0 \ll 1$, but the choice of ϕ_0 is arbitrary and, indeed, ϕ_0 cannot be chosen too small (a possible choice is $\phi_0 = 0.1 - 0.2$), otherwise, in the practical case of a numerical simulation, the band would almost "invade" the surrounding body. But as shown in Sec. 4.2 and illustrated in the example of Sec. 4.3, an application of the proposed closed-path approach removes this ambiguity. This is because the GEM tensor can be evaluated on the closed path *ACBA* that traverses the band defined by the phase field, with no need of defining the locations of points *A* and *B*. The resulting integral results to be path-independent as long as it is taken in a region, like the one envisaged in Fig. 1, where the material is unaffected by the propagation of the tip of the damage band. If the integral is taken in another region, the integral representation accounts only for the energy that is dissipated within the region that is enclosed by the contour. In Sec. 4.4, we show that a modification of the GEM tensor and closed-path integration allows the direct measurement of the energy release rate for the moving band, and the evaluation of the residual elasticity within the band may result after it yields as shown in the model of Ref. [13].

We believe that the proposed method can be applied in many other problems involving *not-neat* separation of the crack surfaces. For example, it could be applied to the measurement of the fracture toughness of *bulk* adhesive joints [17], where small-scale linear elastic fracture mechanics (LEFM) and the traditional *J*-integral cannot account for the large size of the fracture process zone. Other interesting applications could be in the characterization of the mechanical failure of lithium ion battery electrodes [18], through the possibility of taking into account directly the effects of the electric fields traversing cracks [19]. In general, the applicability and the limitations of the closed-path *J*-integral in measuring the effects of dissipative processes still needs to be validated on theoretical grounds [20], but this is beyond the scope of the present article. Nevertheless, we believe that the method proposed here provides a direct link between the mechanics of sharp cracks and its regularized description through damage mechanics.

2 The Eshelby Method for a Bimaterial Elastic Solid

The simplest case that illustrates the use of closed-path contours is that of an elastic solid composed of two materials that are separated by an elastic interphase. In this illustrative example, in the spirit of Eshelby [2] no crack is present. We first define the mechanics of the interphase and then consider the energy dissipation within the interphase and the energy release rate associated its cracklike extension.

2.1 A Paradigmatic Example. Consider an elastic body Ω in generalized plane stress or plane strain, composed of two regions joined by an elastic interface. For simplicity, as represented in Fig. 2(*a*), we assume that the interface is straight and can be represented by a (nonlinear) elastic material with reference thickness *h*. In the following, we will consider the limit in which the thickness of the interface is negligible with respect to the other length-scales of the problem, and we will derive the conclusions in the limit $h \to 0$.

The midline of the elastic interface is supposed to be a line of geometric and elastic symmetry. If the applied loading and boundary conditions are symmetric with respect to the same line, the traction across the interface consists of only a stress component normal to the separation surface. The intensity of the stress is assumed to depend upon the stretch of the surface. In the language of cohesive fracture mechanics, the cohesive forces *per* unit area, say *f*, is a function of the COD, say $2v$, i.e., $f = f[2v]$. At this point, we do not make any assumption about the constitutive equation that describes the elastic interface, other than that it is qualitatively of the type represented in Fig. 2(*b*). There is a threshold $f_0 > 0$ that is necessary to activate the interface, i.e., it takes a stress $f_0 > 0$ to initiate the enlargement of the interface. Such a stress increases up to a maximum f_M corresponding to the relative displacement $2v_M$, beyond which it decreases and becomes null if the enlargement becomes larger than the limit $2v_0$. At this stage, the corresponding portion of the interface is stress-free. This assumption also includes the particular case in which the strain-hardening branch $(0, v_M)$ is evanescent, i.e., $f_M = f_0$, and the constitutive law is monotone decreasing.

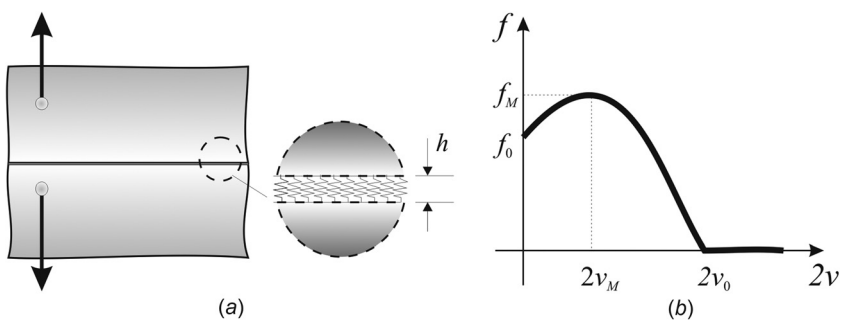

Fig. 2 (*a*) The body composed of two elastic solids joined by a straight elastic interface. (*b*) A general constitutive equation relating the interface-stress with the relative displacement.

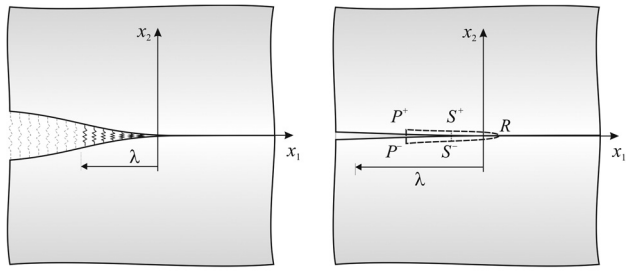

Fig. 3 (*a*) Deformed configuration of the body. (*b*) The closed-path contour for the application of Eshelby energy moment tensor.

Let the system be subject to some external quasi-statically and monotonically applied forces, as schematically represented in Fig. 2(*a*). The body will find an equilibrium configuration that coincides with the solution of the corresponding elasticity problem, under the prescribed conditions at the boundary and jump conditions at the interface. If the constitutive equation is of the type of Fig. 2(*b*), we qualitatively expect a deformation that, as indicated in Fig. 3(*a*), resembles the COD of a cohesive crack. Introduce the reference system (x_1, x_2), with associated unit vectors $(\mathbf{e}_1, \mathbf{e}_2)$, such that the x_1 axis coincides with the symmetry line and the x_2 axis is at right angle to it. Then, define the displacement field components in the form

$$\mathbf{u}(\mathbf{x}) = u_1(x_1, x_2)\mathbf{e}_1 + u_2(x_1, x_2)\mathbf{e}_2 \tag{2.1}$$

The interface will yield according to the resulting stress, and the variation of its thickness will be $2v(x_1) = u_2(x_1, 0^+) - u_2(x_1, 0^+) = 2u_2(x_1, 0^+) = -2\,u_2(x_1, 0^+)$. Here, we have set $\pm h/2 \cong 0^{\pm}$ in the limit $h \to 0$. There will be regions where: (i) the interface is *inactive*, i.e., the stress is less than f_0 and $2v(x_1) = 0$; (ii) the interface is *active*, since $0 < 2v(x_1) < 2v_0$; and (iii) the interface is completely yielded and $2v(x_1) > 2v_0$. Consider an equilibrium state and choose the origin of the axes such that the interface is inactive for $x_1 > 0$, active for $-\lambda < x_1 < 0$ and yielded for $x_1 < -\lambda$. In Fig. 3(*a*), the springs that schematically represent the cohesive interface have been drawn with dashed lines in the region where the interface has yielded.

An energetic potential *per* unit area of the interface can be defined as

$$F[s] = \int_0^s f[\tau]\, d\tau \tag{2.2}$$

Obviously, in the yielded region where $2v_2(x_1, 0^+) > 2v_0$, one has that $F[2v_2(x_1, 0^+)] = F[2v_0] = F_0$. Consider a pseudotriangular closed path P^-P^+R, as represented in Fig. 3(*b*), which is supposed to shrink and in the limit embraces part of the interface. Observe that in the standard application of the *J*-integral, the crack acts as a barrier and, consequently, the path is not supposed to cross the crack surfaces. On the other hand, here there is no crack, and consequently, it is possible to consider a closed path. We can then apply the most general form of the Eshelby theorem (1.2) proposed by Gurtin and Podio-Guidugli [4,5]. For the particular configuration just described, no stress singularity can occur because the state of stress at the interface cannot be higher than f_M. Therefore, in the limit, the point R of Fig. 3(*a*) can tend to the origin of the reference system, i.e., to the boundary between the active and inactive regions. As the path becomes closer to the interface, continuity of the stress implies that

$$\begin{aligned}\sigma_{22}(x_1, 0^+) = \sigma_{22}(x_1, 0^-) &= f[u_2(x_1, 0^+) - u_2(x_1, 0^-)] \\ &= f[2u_2(x_1, 0^+)] = f[-2u_2(x_1, 0^-)]\end{aligned} \tag{2.3}$$

If the active portion advances in the positive direction of the x_1 axis, then the energy release rate of the whole elastic system reads

$$\begin{aligned}J = &\int_{P^+R} (\Psi \mathbf{e}_1 \cdot \mathbf{n} - \mathbf{S}\mathbf{n} \cdot \nabla \mathbf{u}\, \mathbf{e}_1) ds \\ &+ \int_{RP^-} (\Psi \mathbf{e}_1 \cdot \mathbf{n} - \mathbf{S}\mathbf{n} \cdot \nabla \mathbf{u}\, \mathbf{e}_1) ds \\ &+ \int_{P^-P^+} (\Psi \mathbf{e}_1 \cdot \mathbf{n} - \mathbf{S}\mathbf{n} \cdot \nabla \mathbf{u}\, \mathbf{e}_1) ds\end{aligned} \tag{2.4}$$

On the path $P^{\pm}R$, one has that $\mathbf{n} = \pm\mathbf{e}_2$, $\nabla \mathbf{u}\mathbf{e}_1 = \mathbf{e}_1(\partial/\partial x_1)u_1(x_1, 0^{\pm}) + \mathbf{e}_2(\partial/\partial x_1)u_2(x_1, 0^{\pm})$, and $\mathbf{S}\mathbf{n} = \sigma_{22}(x_1, 0^{\pm})\,\mathbf{e}_2$. On the other hand, on P^-P^+ one finds $\mathbf{n} = -\mathbf{e}_1$, $\mathbf{S}\mathbf{n} = 0$, and $\Psi = F[2u_2(x_{1P}, 0^+)]/h$, where x_{1P} denotes the abscissa of points P^- and P^+. Therefore, Eq. (2.4) becomes

$$\begin{aligned}J = &-\int_{P^+R} \sigma_{22}(x_1, 0^+) \frac{\partial}{\partial x_1} u_2(x_1, 0^+) ds \\ &+ \int_{RP^-} \sigma_{22}(x_1, 0^-) \frac{\partial}{\partial x_1} u_2(x_1, 0^-) ds + \int_{P^-P^+} -\Psi ds\end{aligned} \tag{2.5}$$

The first two integrals read

$$\begin{aligned}&-\int_{x_{1P}}^{0^+} \sigma_{22}(x_1, 0^+) \frac{\partial}{\partial x_1} \left(2u_2(x_1, 0^+)\right) dx_1 \\ &= -\int_{x_{1P}}^{0^+} f\left[2u_2(x_1, 0^+)\right] \frac{\partial}{\partial x_1} \left(2u_2(x_1, 0^+)\right) dx_1 \\ &= -\int_{2u_2(x_{1P}, 0^+)}^{0} f\left[2u_2(x_1, 0^+)\right] d\left(2u_2(x_1, 0^+)\right) \\ &= \int_0^{2u_2(x_{1P}, 0^+)} f[\tau] d\tau = F\left[2u_2(x_{1P}, 0^+)\right]\end{aligned} \tag{2.6}$$

whereas the third integral takes the form

$$\begin{aligned}\int_{P^-P^+} \Psi \mathbf{e}_1 \cdot \mathbf{n} ds &= \int_{P^-P^+} -\Psi ds \\ &= -\int_{P^-P^+} \frac{F[2u_2(x_{1P}, 0^+)]}{h} ds \\ &= -F\left[2u_2(x_{1P}, 0^+)\right]\end{aligned} \tag{2.7}$$

The conclusion is that $J = 0$, independently of the crack path, in agreement with Eshelby's theorem. Note, in fact, that the derivation of Eqs. (2.6) and (2.7) is independent of whether the path P^-P^+ traverses either the active or the yielded regions. In terms of fracture mechanics, this finding is in agreement with the condition that crack extension initiates when the energy release rate equals the energy dissipated in the cohesive zone. Recall, in fact, that a crucial assumption in the derivation of Eqs. (2.6) and (2.7) is that the whole system is in elastic equilibrium.

Note that one could use the same argument on any pillow path $P^-P^+\,S^+S^-$, of the type represented in Fig. 3(*b*), to find that the corresponding integral of the energy momentum tensor vanishes. This is true, regardless of the location of the branches P^-P^+ and S^-S^+, identified by the abscissas x_{1P} and x_{1Q}.

2.2 Interfacial Dissipation and Energy Release Rate. It is instructive to sort and interpret the contributions of the three integrals appearing in Eq. (2.5). This can be done on the basis of a classical argument. Suppose the interface tip moves by an amount ξ in the x_1 direction, so that a new equilibrium state is attained. If,

following the same hypothesis for cohesive cracks of Ref. [9], the length λ of the active region is much smaller than the length of the whole interface, i.e., λ is much smaller than the reference length scales associated with the elastic problem, then the deformed shape remains unchanged. This means that the u_2 component of the new displacement field will be such that $u_{2\xi}(x_1, 0^{\pm}) = u_2(x_1 - \xi, 0^{\pm})$. In the energetic variation of the whole system, the contribution associated with the interface only is

$$\Delta\Lambda(\xi) = \int_{-L}^{l} F[2u_2(x_1 - \xi, 0^+)] - F[2u_2(x_1, 0^+)]\, dx_1 \tag{2.8}$$

where we have assumed that $L > \lambda$ and $l > \xi$. In fact, outside the interval $-L \le x_1 \le l$, the static state of the interface does not change. Therefore, the rate of change of the interfacial energy at $\xi = 0$ reads

$$\begin{aligned}
&\frac{d}{d\xi}(\Delta\Lambda(\xi))_{\xi=0} \\
&= \left\{ \int_{-L}^{l} f\left[2u_2\left(x_1 - \xi, 0^+\right)\right] \frac{\partial}{\partial \xi}\left(2u_2\left(x_1 - \xi, 0^+\right)\right) dx_1 \right\}_{\xi=0} \\
&= \left\{ \int_{-L}^{l} -f\left[2u_2\left(x_1 - \xi, 0^+\right)\right] \frac{\partial}{\partial x_1}\left(2u_2\left(x_1 - \xi, 0^+\right)\right) dx_1 \right\}_{\xi=0} \\
&= \int_{-\lambda}^{0} -f\left[2u_2\left(x_1, 0^+\right)\right] d\left(2u_2\left(x_1, 0^+\right)\right) \\
&= -2\int_{2v_0}^{0} f[\tau] d(\tau)\, dx_1 = F[2v_0] = 2F_0
\end{aligned} \tag{2.9}$$

This represents the work that has to be expended to let the yielded interface advance by $d\xi$ from $\xi = 0$, divided by $d\xi$. This contribution is the opposite of Eq. (2.7) because, in the words of Ref. [2], the term (2.7) represents the energy that is *added* to the reference domain enclosed by the path P^-P^+R when, thinking of keeping fixed the interface, the domain is moved in the direction of increasing ξ. Since in this case, the energy is *subtracted*, a negative sign appears in Eq. (2.7).

The work required to yield the interface must be provided by the energy release rate of the elastic matrix that surrounds the interface itself. In general, the body is subjected to dead-load tractions on the boundary, so that it is convenient to refer to the complementary energy $U[\boldsymbol{t}]$, where $\boldsymbol{t}$ denote the boundary tractions. It is convenient to consider distinctly the two elastic sub-bodies that are joined by the interface and define for each portion the complementary energies $U^+[\boldsymbol{t}]$ and $U^-[\boldsymbol{t}]$, where the superscripts refer to the part that is located in the direction of the positive or negative x_2 axis. Let $q(x_1, 0^+) = \sigma_{22}(x_1, 0^+)$ and $q(x_1, 0^-) = \sigma_{22}(x_1, 0^-)$ represent the tractions that are applied to the two sub-bodies through the interface. Equilibrium provides $q(x_1, 0^+) = q(x_1, 0^-) = q(x_1)$, and Castigliano's theorem states

$$\frac{\partial U^+}{\partial q(x_1, 0^+)} = -u_2\left(x_1, 0^+\right), \quad \frac{\partial U^-}{\partial q(x_1, 0^-)} = u_2(x_1, 0^-) \tag{2.10}$$

When the yielded portion of the interface moves, then the traction becomes $q_\xi(x_1, 0^+) = q_\xi\,(x_1, 0^-)$ and, if the shape of the interface profiles does not change, then $q_\xi(x_1, 0^+) = q(x_1 - \xi, 0^+)$ and $q_\xi(x_1, 0^-) = q(x_1 - \xi, 0^-)$. Then, the rate of change of the complementary energy for a movement of the yielded interface in the positive ξ direction reads

$$\begin{aligned}
\frac{d}{d\xi}(\Delta\Theta(\xi))_{\xi=0} &= \frac{d}{d\xi}\left\{ \int_{-L}^{l} \left(U\left[q_\xi\left(x_1, 0^+\right)\right] + U[q_\xi(x_1, 0^-)]\right) dx_1 \right\}_{\xi=0} \\
&= \left\{ \int_{-L}^{l} \left(-u_{2\xi}\left(x_1, 0^+\right) \frac{\partial}{\partial \xi} q\left(x_1 - \xi, 0^+\right) + u_2(x_1, 0^-) \frac{\partial}{\partial \xi} q(x_1 - \xi, 0^-) \right) dx_1 \right\}_{\xi=0} \\
&= \int_{-L}^{l} \left(u_2\left(x_1, 0^+\right) - u_2(x_1, 0^-)\right) \frac{\partial}{\partial x_1} q(x_1) dx_1 = \left[\left(u_2\left(x_1, 0^+\right)\sigma_{22}\left(x_1, 0^+\right) - u_2(x_1, 0^-)\sigma_{22}(x_1, 0^-)\right)\right]_{-L}^{l} \\
&\quad - \int_{-\lambda}^{0} \left(\sigma_{22}\left(x_1, 0^+\right) \frac{\partial}{\partial x_1}\left(u_2\left(x_1, 0^+\right)\right) - \sigma_{22}(x_1, 0^-) \frac{\partial}{\partial x_1} u_2(x_1, 0^-) \right) dx_1 \\
&= -\int_{-\lambda}^{0} \sigma_{22}\left(x_1, 0^+\right) \frac{\partial}{\partial x_1}\left(u_2\left(x_1, 0^+\right)\right) dx_1 + \int_{-\lambda}^{0} \sigma_{22}(x_1, 0^-) \frac{\partial}{\partial x_1}\left(u_2(x_1, 0^-)\right) dx_1
\end{aligned} \tag{2.11}$$

In writing Eq. (2.11), we have used the fact that $\sigma_{22}(-L, 0^+) = 0$ and $u_2\ (l, 0^+) - u_2(l, 0^-) = 0$. Since the complementary energy evaluated on the elastic solution equals the opposite of the total potential energy, then Eq. (2.11), which is equal to the first two integrals of Eq. (2.5), represents a positive quantity equal to the energy release rate in the elastic matrix. Such a value coincides with that found in Ref. [6] as a direct application of the J-integral on a closed contour that embraces the cohesive forces.

The conclusions just reached correspond to the case in which, in the evaluation of the integral of Eq. (2.4), the path P^-P^+R is such that $x_{1P} < -\lambda$ and $x_{1R} > 0$, i.e., the whole yielded portion of the interface is embraced by the contour. It is much more interesting to repeat the same argument by considering the pillow path $P^-P^+\ S^+S^-$ of Fig. 3(*b*), where the abscissas x_{1R} and x_{1S} can be *anywhere* along the interface. Reasoning as in Eq. (2.9), one finds that

$$\begin{aligned}
&\int_{P^-P^+} \boldsymbol{\Psi}\mathbf{e}_1 \cdot \mathbf{n} ds + \int_{S^-S^+} \boldsymbol{\Psi}\mathbf{e}_1 \cdot \mathbf{n} ds \\
&\quad = -\int_{P^-P^+} \frac{F[2u_2(x_1, 0^+)]}{h} ds + \int_{S^-S^+} \frac{F[2u_2(x_1, 0^+)]}{h} ds \\
&\quad = -F\left[2u_2\left(x_{1P}, 0^+\right)\right] + F\left[2u_2\left(x_{1S}, 0^+\right)\right]
\end{aligned} \tag{2.12}$$

This equals *minus* the work rate to be expended on the portion $x_{1P} \le x_1 \le x_{1P}$ of the interface as it is moved in the positive ξ direction. On the other hand, with the same derivation of Eq. (2.11), one has

$$-\int_{P^+S^+}\sigma_{22}(x_1,0^+)\frac{\partial}{\partial x_1}u_2(x_1,0^+)ds + \int_{P^-S^-}\sigma_{22}(x_1,0^-)\frac{\partial}{\partial x_1}u_2(x_1,0^-)ds = \frac{d}{d\xi}\left\{\int_{x_{1P}}^{x_{1S}}\left(U\left[q_\xi(x_1,0^+)\right]+U[q_\xi(x_1,0^-)]\right)dx_1\right\}_{\xi=0} \tag{2.13}$$

This contribution equals the energy release rate in the elastic matrix associated with the movement of the interface, but it is restricted to only the portion $x_{1P}\le x_1\le x_{1P}$. The physical significance of such a "restriction" is stated, in the sense of Castigliano's theorem, by the intervals of integration in the right-hand side term of the equality (2.13).

3 Closed-Path J-Theory for Fractures

The method just proposed for elastic interfaces is now extended to bridged cracks.

3.1 Self-Similarity of Crack Profiles. A key hypothesis that allowed the development of the arguments of Sec. 2 and that will be used again in Sec. 3 is that the shape of the interface profile does not change during the advancement of the yielded portion. Here, we derive the condition according to which the crack tip region does not alter its shape during its advancement. Consider the plane problem of a straight crack opening in mode I, traversing an infinite, homogeneous and isotropic, elastic medium, with shear modulus G, Poisson's ratio ν, and Young's modulus $E=2\ G\ (1+\nu)$. The crack tip occupies the position $x_2=0$, $x_1\le 0$. It is convenient to consider the case of a pressurized crack, for which the crack opening pressure is $p(x_1)$. Denote by $q(x_1)$ the bridging forces that oppose $p(x_1)$ and resist the COD. The COD can be determined using the weight function method and written as

$$u_2(x_1,0^\pm)=\pm\int_{-\infty}^{0}(p(\tau)-q(\tau))\,m(x_1,\tau)d\tau \tag{3.1}$$

If the process of crack advancement occurs at a length scale much smaller than the characteristic length scales of the physical problem, one can use the solution of a semi-infinite crack, which for plane strain reads

$$m(x_1,\tau)=\frac{1-\nu}{\pi G}\log\frac{\sqrt{-x_1}+\sqrt{-\tau}}{\left|\sqrt{-x_1}-\sqrt{-\tau}\right|} \tag{3.2}$$

Suppose that the crack advances by ξ in the positive x_1 direction. The bridging forces and the crack surface displacements become, respectively, $q_\xi(x_1)$ and $u_{2\xi}(x_1,0^\pm)$. It is customary to suppose that such quantities are related by a constitutive equation of the type $q_\xi(x_1)=f[2u_{2\xi}(x_1,0^+)]$. This is analogous to $f=f[2v]$ of Eq. (2.3), and we can still suppose that the trend is similar to that of Fig. 2(*b*). On the other hand, the form of the opening pressure $p(x_1)$ when the crack advances, i.e., for $0\le x_1\le\xi$, clearly depends upon the conditions on the far boundary (the applied loads). We intend to find conditions for the existence of a self-similar solution, that is, a solution for which the bridging forces and the CODs become, respectively, $q_\xi(x_1)=q\ (x_1-\xi)$ and $u_{2\xi}(x_1,0^\pm)=u_2(x_1-\xi,0^\pm)$ in a neighborhood of $\xi=0^+$. Supposing that $q_\xi(x_1)=q\ (x_1-\xi)$, then one has

$$u_{2\xi}(x_1,0^\pm)=\pm\int_{-\infty}^{\xi}(p(\tau)-q(\tau-\xi))\,m(x_1-\xi,\tau-\xi)d\tau \tag{3.3}$$

and, differentiating

$$\begin{aligned}\frac{\partial}{\partial\xi}\left(u_{2\xi}(x_1,0^+)\right)_{\xi=0} &= \frac{\partial}{\partial\xi}\left\{\int_{-\infty}^{\xi}\left(p(\tau)-q(\tau-\xi)\right)m(x_1-\xi,\tau-\xi)\,d\tau\right\}_{\xi=0}\\ &= \left(p(0)-q(0)\right)m(x_1,0)+\int_{-\infty}^{0}q'(\tau)m(x_1,\tau)\,d\tau\\ &\quad-\int_{-\infty}^{0}(p(\tau)-q(\tau))\frac{\partial}{\partial x_1}m(x_1,\tau)\,d\tau\\ &\quad-\int_{-\infty}^{0}(p(\tau)-q(\tau))\frac{\partial}{\partial\tau}m(x_1,\tau)\,d\tau\end{aligned} \tag{3.4}$$

Integrating by parts the last integral and observing from Eq. (3.2) that $m(x_1,0)=m(x_1,-\infty)=0$, the final result is

$$\begin{aligned}\frac{\partial}{\partial\xi}\left(u_{2\xi}(x_1,0^+)\right)_{\xi=0} &= -\int_{-\infty}^{0}(p(\tau)-q(\tau))\frac{\partial}{\partial x_1}m(x_1,\tau)\,d\tau\\ &\quad+\int_{-\infty}^{0}p'(\tau)m(x_1,\tau)\,d\tau\\ &= -\frac{\partial}{\partial x_1}\left(u_2(x_1,0^+)\right)+\int_{-\infty}^{0}p'(\tau)m(x_1,\tau)\,d\tau\end{aligned} \tag{3.5}$$

An analogous representation holds for $u_{2\xi}(x_1,0^-)$. Consequently, one obtains that $u_{2\xi}(x_1,0^\pm)=u_2(x_1-\xi,0^\pm)$ provided that

$$\int_{-\infty}^{0}p'(\tau)m(x_1,\tau)\,d\tau=0 \tag{3.6}$$

In principle, this condition would rule out, for example, the important case in which the crack is orthogonal to the axis of a beam under flexure; for this case, $p'(x_1)=\text{const.}\neq 0$. However, an estimation of the order of magnitude of this term indicates that, unless there is a strong variation in $p(x_1)$ at $x_1=0$, it provides a second-order contribution especially when the length of the crack is much smaller than the reference length-scale of the problem. In other words, self-similarity is a consequence of the fact that the opening is universal near the crack tip in terms of asymptotic Williams solution.

3.2 Closed J-Path Integral Theory for Bridged Cracks: The Small-Scale Bridging Limit. Consider a generic closed path $P^-P^+S^+S^-$ as represented in Fig. 3(*b*). This figure, recalling the case of an elastic interface, is also representative of a bridged crack since the schematic representation is essentially the same. Let the cohesive forces *per* unit area be constitutively regulated by $f=f[2v]$ of the COD $2v$. An argument completely identical to that of Sec. 2.1 shows that, under self-similarity of the crack tip profile

$$J=-\int_{P^+S^+}\sigma_{22}(x_1,0^+)\frac{\partial}{\partial x_1}u_2(x_1,0^+)ds + \int_{P^-S^-}\sigma_{22}(x_1,0^-)\frac{\partial}{\partial x_1}u_2(x_1,0^-)ds+\int_{P^-P^+}-\Psi ds + \int_{S^-S^+}\Psi ds=0 \tag{3.7}$$

In other words, the closed-path J-integral is zero. We emphasize that the integral is evaluated on a closed contour, unlike in the classical derivation of Ref. [6] in which the branches P^-P^+ and S^+S^- are missing because the crack is considered as a barrier.

Introducing the potential $F[2v]$ of the cohesive forces, defined similarly to Eq. (2.2), the last two integrals of Eq. (3.7) take the form

$$\int_{P^-P^+} -\Psi ds + \int_{S^-S^+} \Psi ds = -F[2u_2(x_{1P}, 0^+)] + F[2u_2(x_{1S}, 0^+)] \tag{3.8}$$

meaning that the integrals on the branches account for the energy associated with the cohesive forces per unit area while traversing the crack. It should be noted that the traversing branches may intersect portions of the cracks where the cohesive forces are null, i.e., where either the COD is null or the COD is greater than the critical limit $2v_0$. Using the same notation as Eq. (2.2), in the first case the corresponding potential in Eq. (3.8) is null, whereas in the second case it is equal to $2F_0$. In general, $F[2u_2(x_{1P}, 0^+)]$ and $F[2u_2(x_{1S}, 0^+)]$ take a value between 0 and $2F_0$.

With no modification, this approach can readily account for the ACK limit of bridged cracks [21], so named after the seminal work by Aveston Kooper and Kelly [22]. This condition corresponds to a case in which the COD takes a constant value in the wake of the crack at distances relatively far from the crack tip. Such a limit can exist if the remotely applied load is uniform, so that constant bridging tractions are required to balance the applied loads, and only if the function $f[2v]$ has an initial strain-hardening branch [21].

For the interpretation of the first two integrals of Eq. (3.7), imagine that the applied loads are kept constant. Introduce then, similarly to what was done in Sec. 2.2, the complementary energy function $U[\boldsymbol{t}]$, where $\boldsymbol{t}$ represents the boundary tractions on the crack surface. Let $q(x_1, 0^+) = \sigma_{22}(x_1, 0^+)$ and $q(x_1, 0^-) = \sigma_{22}(x_1, 0^-)$ denote the tractions applied along the upper and lower crack surfaces. These are related with the complementary energy functional by Castigliano's theorem, as per Eq. (2.10). Since $q(x_1, 0^+) = q(x_1, 0^-) = q(x_1)$, the complementary energy can be restated in terms of $q(x_1)$ only, so that

$$\frac{\partial U}{\partial q(x_1)} = -\left(u_2\left(x_1, 0^+\right) - u_2(x_1, 0^-)\right) = -2u_2\left(x_1, 0^+\right) = 2u_2(x_1, 0^-) \tag{3.9}$$

Then, reasoning as in Eq. (2.11), one finds

$$-\int_{x_{1P}}^{x_{1S}} \sigma_{22}\left(x_1, 0^+\right) \frac{\partial}{\partial x_1}\left(u_2\left(x_1, 0^+\right)\right) dx_1 + \int_{x_{1P}}^{x_{1P}} \sigma_{22}(x_1, 0^-) \frac{\partial}{\partial x_1}(u_2(x_1, 0^-))\, dx_1 = \int_{x_{1P}}^{x_{1S}} \dot{U}[q(x_1)]\, dx_1 \tag{3.10}$$

where we have synthetically posed

$$\dot{U}[q(x_1)] = \lim_{\xi \to 0} \frac{U[q(x_1 - \xi)] - U[q(x_1)]}{\xi} = -2u_2\left(x_1, 0^+\right) \lim_{\xi \to 0} \frac{q(x_1 - \xi) - q(x_1)}{\xi} \tag{3.11}$$

This contribution represents the energy release rate that is associated only with the work done by the cohesive forces acting in the interval $x_{1P} \le x_1 \le x_{1S}$, during a self-similar movement of the crack profile.

It is interesting to consider as well the *small-scale bridging limit*, a condition in which the length λ of the cohesive zone is infinitesimal with respect to the length of the crack. Referring again to Fig. 3(*b*), consider a generic closed path $P^-P^+S^+S^-$ such that $x_{1P} < -\lambda$ and $x_{1S} > 0$. Consider then the same closed-path J-integral of Eq. (3.7). It is possible to show [23] that, in plane strain conditions, one has

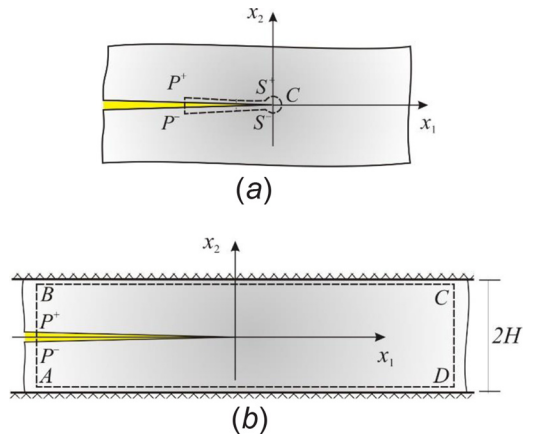

Fig. 4 (*a*) Closed-path contour for a crack with a tip stress singularity. (*b*) A special configuration for which the contour integral J can be readily evaluated.

$$\lim_{\lambda \to 0} \int_{x_{1P}}^{x_{1S}} \left\{ -\sigma_{22}\left(x_1, 0^+\right) \frac{\partial}{\partial x_1}\left(u_2\left(x_1, 0^+\right)\right) + \sigma_{22}(x_1, 0^-) \frac{\partial}{\partial x_1}(u_2(x_1, 0^-)) \right\} dx_1 = \lim_{\lambda \to 0} \int_{-\lambda}^{0} \left\{ -\sigma_{22}\left(x_1, 0^+\right) \frac{\partial}{\partial x_1}\left(u_2\left(x_1, 0^+\right)\right) + \sigma_{22}(x_1, 0^-) \frac{\partial}{\partial x_1}(u_2(x_1, 0^-)) \right\} dx_1 = (1 - \nu) \frac{K_I^2}{2G} \tag{3.12}$$

where K_I is the stress intensity factor for mode I crack opening. On the other hand, using the same argument of Eq. (3.8), one finds

$$\lim_{\lambda \to 0} \left(\int_{P^-P^+} -\Psi ds + \int_{S^-S^+} \Psi ds \right) = \lim_{\lambda \to 0} \left(\int_{P^-P^+} -\Psi ds \right) = -F[2v_0] = -\gamma_0 \tag{3.13}$$

where using a classical notation in LEFM, we have indicated with γ_0 the energy necessary to produce the fracture *per* unit of fractured surface.

The fact that the closed-path J-integral of Eq. (3.7) takes the null value is then analogous to the classical energetic balance *à la* Griffith.

Thinking of the small-scale bridging limit, one can also directly evaluate the closed-path J-integral in the case of a sharp crack. One of the possible contours to be considered is of the type represented in Fig. 4(*a*), where the path $P^-P^+S^+S^-$, with $x_{1S} \to 0^-$, is completed with a small circle C enclosing the crack tip, to avoid the stress singularity here present.

In the limit in which the contour shrinks on the crack profile, the only non-null contributions come from the branch P^-P^+ and from the circle C because no forces are applied on the crack surfaces. Reasoning as in Eq. (3.13), the integral on P^-P^+ gives the contribution $-\gamma_0$; the integral on C gives the same result of Eq. (3.12). Therefore, formally one has

$$J = \int_{P^-P^+C S^+S^-} (\Psi \mathbf{e}_1 \cdot \mathbf{n} - \mathbf{S}\mathbf{n} \cdot \nabla \mathbf{u}\, \mathbf{e}_1) ds = \int_{P^-P^+} -\Psi ds - \int_C \mathbf{S}\mathbf{n} \cdot \nabla \mathbf{u}\, \mathbf{e}_1 ds = -\gamma_0 + \frac{1 - \nu}{2G} K_I^2 = 0 \tag{3.14}$$

Of course, using well-known arguments, it is possible to demonstrate that the closed-path J-integral always vanishes, whatever the closed contour considered traverses or does not traverse the barrier represented by the material discontinuity.

3.3 Cohesive Versus Bridged Cracks. In general, a "bridged crack" is characterized by tractions that oppose the COD. The bridging actions may be classified into two distinct categories: (i) those operating at the small scale, in a neighborhood of the crack tip and (ii) those associated with large COD in the crack wake. The contribution (i) involves bridging stresses of the same order of the elastic modulus of the material that are related with the strong interaction of the material constituent particles, whereas (ii) is often associated with a weaker source such as, for example, the action of fibers embedded in the elastic matrix.

The two effects can certainly be treated simultaneously, but it is useful to distinguish their two sources. An effective way to do this is to consider the small-scale bridging limit for the cohesive forces of (i) and maintain the distributed character of the interaction of type (ii) in the crack wake. The result is a configuration in which there are distributed cohesive forces along the crack, but the crack tip stress intensity factor is *not* null. It is customary to refer to this scenario as the *bridged-crack model*, to distinguish it from a *cohesive zone model*, where the stress intensity factor vanishes [21].

The closed-path J-integral can be applied to this configuration with no major variation with respect to what has been presented so far. Suppose that the force per unit area $f[2v]$ and the corresponding potential $F[2v]$ of Eq. (2.2) are associated with the *only* contribution of the type (ii). Consider again the path $P^-P^+CS^+S^-$, of the same type as that of Fig. 4(*a*), and calculate the J-integral in the form

$$\begin{aligned} J &= \int_{P^-P^+CS^+S^-} (\Psi \mathbf{e}_1 \cdot \mathbf{n} - \mathbf{S}\mathbf{n} \cdot \nabla \mathbf{u}\, \mathbf{e}_1) ds \\ &= \int_{P^-P^+} -\Psi ds - \int_{P^+S^+} f\left[2u_2(x_1, 0^+)\right] \frac{\partial}{\partial x_1} u_2(x_1, 0^+) ds \\ &\quad + \int_{P^-S^-} f\left[2u_2(x_1, 0^+)\right] \frac{\partial}{\partial x_1} u_2(x_1, 0^+) ds - \int_C \mathbf{S}\mathbf{n} \cdot \nabla \mathbf{u}\, \mathbf{e}_1 ds = 0 \end{aligned} \tag{3.15}$$

Using the same argument of Eq. (2.9), one has

$$\begin{aligned} &-\int_{P^+S^+} f\left[2u_2(x_1, 0^+)\right] \frac{\partial}{\partial x_1} u_2(x_1, 0^+) ds \\ &\quad + \int_{P^-S^-} f\left[2u_2(x_1, 0^+)\right] \frac{\partial}{\partial x_1} u_2(x_1, 0^+) ds = 2F\left[2u_2(x_{1P}, 0^+)\right] \end{aligned} \tag{3.16}$$

Moreover, comparing with Eq. (3.14) one finds

$$\begin{aligned} &\int_{P^-P^+} -\Psi ds - \int_C \mathbf{S}\mathbf{n} \cdot \nabla \mathbf{u}\, \mathbf{e}_1 ds \\ &\quad = -2F\left[2u_2(x_{1P}, 0^+)\right] - \gamma_0 + \frac{1-\nu}{2G} K_I^2 \end{aligned} \tag{3.17}$$

Since the value of the J-integral on a closed path is independent of the path itself, comparing with Eqs. (3.15), (3.16), and (3.17), an effective way to calculate the stress intensity factor in a bridged crack comes from the identity

$$\frac{(1-\nu)}{2G} K_I^2 = \gamma_0 = J^* = \int_\Gamma (\Psi^* \mathbf{e}_1 \cdot \mathbf{n} - \mathbf{S}\mathbf{n} \cdot \nabla \mathbf{u}\, \mathbf{e}_1) ds \tag{3.18}$$

Here, Γ is again any *closed* path embracing the crack tip, whereas we have indicated with Ψ^* the *effective* strain energy, which coincides with the elastic strain energy in the bulk part of the body, whereas it is represented by the only potential $F[2v]$, associated with the bridging forces of type (ii) when traversing the crack discontinuity. In other words, with respect to Eq. (3.17), we are not considering the contribution γ_0 while crossing the crack discontinuity.

In order to illustrate the potential benefit of the method, consider an elementary example that is the counterpart, for bridged cracks, of a case presented in Ref. [6]. As indicated in Fig. 4(*b*), an infinite strip of height $2H$ is traversed by a semi-infinite central crack, and the loads are applied by clamping the upper and lower surfaces and displacing them apart by an amount 2Δ. The crack is bridged by forces per unit area obeying to the constitutive equation $f = f[2v]$, with corresponding potential $F[2v]$. Let Γ be the dashed *closed* contour AP^-P^+BCD represented in the same figure. Since the u_2 component of displacement is null on the clamped surfaces, the only nonzero contributions come from the paths AP^-, P^-P^+, P^+B, and CD. One thus finds

$$J^* = -\int_{AP^-} \Psi^* ds - \int_{P^-P^+} \Psi^* ds - \int_{P^+B} -\Psi^* ds + \int_{CD} \Psi^* ds \tag{3.19}$$

The strip is infinite and the branches AB and CD are taken to be sufficiently far from the crack tip within which the strain is a uniform value ε_{22}. On CD, one clearly has $\varepsilon_{22} = \Delta/H$, whereas on AP^- and P^+B, indicating with $2u_2(x_{1P}, 0^+)$ the COD at $x_1 = x_{1P}$, the results comes from the solution of the system of equations

$$2G \frac{1-\nu}{1-2\nu} \varepsilon_{22} = f\left[2u_2(x_{1P}, 0^+)\right], \quad \varepsilon_{22} 2H + 2u_2(x_{1P}, 0^+) = 2\Delta \tag{3.20}$$

Therefore, Eq. (3.19) becomes

$$\begin{aligned} J^* &= \frac{1}{2} G \frac{2(1-\nu)}{(1-2\nu)} \left(-\varepsilon_{22,AB}^2 + \varepsilon_{22,CD}^2\right) 2H - F\left[2u_2(x_{1P}, 0^+)\right] \\ &= \frac{1-\nu}{2G} K_I^2 \end{aligned} \tag{3.21}$$

In the simplest case in which $f[\cdot]$ is a linear function, i.e., $f = \kappa \cdot 2v$, one obtains

$$\frac{1-\nu}{2G} K_I^2 = J^* = \frac{\left(\frac{2(1-\nu)}{1-2\nu} G\right)^2}{\frac{2(1-\nu)}{1-2\nu} G + \kappa 2H} \frac{\Delta^2}{H} \tag{3.22}$$

Clearly, when $\kappa \to 0$ the same result of Ref. [6] is recovered.

4 Application to Phase-Field Crack Models

The closed contour J-integral approach is especially useful in phase-field models of brittle fracture. This is because in phase-field fractures there is no completely broken material, but instead cracks are modeled as localized bands with high strains that evolve the stiffness from the value associated with the pristine material to null. Among the various formulations that have been proposed, a class of models presents similarities with bridged cracks because a residual elastic stiffness is assumed to remain in the narrow bands regardless of the damage that is accumulated there. Such contribution is usually introduced to stabilize the numerical solution of the problem, but it can have a significant effect on the mechanics of crack propagation.

4.1 Energetic Derivation of Phase-Field Models for Bridged Cracks. The characteristic feature of phase-field models is the presence of an order parameter ϕ, referred to as the *phase field*, which quantifies the level of damage and takes the value $\phi = 1$ in the sound (undamaged) material, and the value $\phi = 0$ where the material is completely damaged (broken). An evolution equation for this parameter is assumed that makes the damage evolve toward a relatively narrow band where the strain localizes. Although not always possible, especially when rate-dependent effects are important [10], a convenient way to derive phase-field model for crack propagation is through a variational approach. There are many

possible ways of defining the corresponding energy functional; here, we will explicitly consider strains energy densities of the type

$$\Theta[\mathbf{u},\phi] = w(\nabla\phi) + g(\phi)\left(\frac{1}{2}\mathbf{C}\nabla^s\mathbf{u}\cdot\nabla^s\mathbf{u} - \frac{\gamma}{2l}\right) + \frac{\gamma}{2l} + h(\phi)\frac{1}{2}\mathbf{C}\nabla^s\mathbf{u}\cdot\nabla^s\mathbf{u} \tag{4.1}$$

where ϕ: $\Omega\rightarrow[0,1]$ denotes the phase field, $\mathbf{u}$: $\Omega\rightarrow\mathrm{R}^d$ is again the displacement field (d is the dimension where the problem is set), $\mathbf{C}$: Sym→Sym is the elasticity tensor, l is a characteristic length scale, and γ is a parameter that, as it will result clear later on, is associated with the fracture energy *per* unit area. The functions $w(\cdot)$, $g(\cdot)$, and $h(\cdot)$ take different values according to the proposed model. In general, for the consistency of the approach, it is necessary to assume

$$\begin{aligned} &w(\cdot)\ \text{convex and superlinear};\ g(0)=0,\ g(1)=1,\ g'(1)=0;\\ &h(0)=h(1)=0;\ 0\le 1-g(\phi)\le 1+h(\phi) \end{aligned} \tag{4.2}$$

Moreover, for convenience, it is useful to refer to a homogenous isotropic elastic solid by setting

$$\frac{1}{2}\mathbf{C}\nabla^s\mathbf{u}\cdot\nabla^s\mathbf{u} = \frac{1}{2}\left[\lambda(\mathbf{I}\cdot\nabla^s\mathbf{u})^2 + 2\mu\nabla^s\mathbf{u}\cdot\nabla^s\mathbf{u}\right] \tag{4.3}$$

where λ and μ are the Lame's constants.

In the KKL model studied by Karma et al. [11], later developed in Ref. [12], the authors proposed $h(\phi)=0$, $g(\phi)=4\ \phi^3-3\ \phi^4$, whereas in the approach by Boudin et al. [13] the choice is

$$\begin{aligned} w(\nabla\phi) &= \frac{1}{2}\gamma l|\nabla\phi|^2, \quad g(\phi) = 1-(1-\phi)^2,\\ h(\phi) &= \phi^2 - 1 + (1-\phi)^2 + \varepsilon \end{aligned} \tag{4.4}$$

In the second approach, the quantity ε is introduced into the elastic part of the energy in order to stabilize the numerical solution of boundary value problems.

The stress tensor $\mathbf{S}$, dual in energy to $\nabla^s\mathbf{u}$, and the vector $\boldsymbol{\omega}$, dual in energy to $\nabla\phi$ and in the following referred to as the "*field vector*," respectively, read:

$$\begin{aligned} \mathbf{S} &= \frac{\partial\Theta}{\partial\nabla^s\mathbf{u}} = (g(\phi)+h(\phi))\left(\lambda(\mathbf{I}\cdot\nabla^s\mathbf{u})\mathbf{I} + 2\mu\nabla^s\mathbf{u}\right),\\ \boldsymbol{\omega} &= \frac{\partial\Theta}{\partial\nabla\phi} = \gamma l\nabla\phi \end{aligned} \tag{4.5}$$

The variational problem to be considered is

$$\min_{(u,\phi)\in A}\int_\Omega \Theta[\mathbf{u},\phi]\,d\mathbf{x} \tag{4.6}$$

where A denotes the class of admissible functions. In general, it is required that $\mathbf{u}$ and ϕ and their first derivatives are square-summable functions in Ω. Traditional geometric or natural boundary conditions are assumed on the border $\partial\Omega$ for the displacement field $\mathbf{u}$. With respect to the phase field, the natural boundary condition is readily found to be $\nabla\phi\cdot\mathbf{n}=0$ on $\partial\Omega$; this applies where the value of ϕ is not specified. Minimizers are sought under conditions equivalent to the *irreversibility* of crack propagation. To do so, the load history is divided into n steps $i=1,\ldots,n$, and the minimization at each step is performed under the constraint that $\phi_i(\mathbf{x})\le\phi_{i-1}(\mathbf{x})$, $\forall\mathbf{x}\in\Omega$ [24].

The governing equations are the corresponding Euler–Lagrange equations of the minimization problem, which read

$$\begin{aligned} &\mathrm{Div}\,\mathbf{S} = 0,\\ &\mathrm{Div}\boldsymbol{\omega} = \frac{\partial\Theta}{\partial\phi} = \left(g'(\phi)+h'(\phi)\right)\frac{1}{2}\left(\lambda(\mathbf{I}\cdot\nabla^s\mathbf{u})^2 + 2\mu\nabla^s\mathbf{u}\cdot\nabla^s\mathbf{u}\right)\\ &\qquad - g'(\phi)\frac{\gamma}{2l} \end{aligned} \tag{4.7}$$

It is essential that the quantity ε in $h(\phi)$ of Eq. (4.4) is not zero to assure that the minimization problem is well-posed, but it is customary to consider it as "small" or "negligible." This is probably due to a result of variational convergence for the minimization problem (4.6), referred to in the Introduction. In fact, by setting

$$\varepsilon = \chi\left(\frac{l(\lambda+2\mu)}{\gamma}\right) \tag{4.8}$$

it can demonstrated that if $\chi(\cdot)$ is a function infinitesimal of order greater than 1, then for $l\rightarrow 0$ the variational problem (4.6) converges [25], in the sense of variational Γ-convergence, to a more classical functional associated with an energetic balance *à la* Griffith. In particular, the result is

$$\min_{(\mathbf{u},\phi)\in A}\int_\Omega \Theta[\mathbf{u},\phi]\,d\mathbf{x} \overset{\Gamma}{\underset{l\rightarrow 0}{\rightarrow}} \min_{\mathbf{u}\in A^{**}}\left\{\int_{\Omega\setminus S[\mathbf{u}]}\frac{1}{2}\mathbf{C}\nabla^s\mathbf{u}\cdot\nabla^s\mathbf{u}\,d\mathbf{x} + \gamma\,\mathrm{meas}\,(S[\mathbf{u}])\right\} \tag{4.9}$$

Here, $S[\mathbf{u}]$ denotes the set of points where $\mathbf{u}$ is discontinuous (the jump points of the field $\mathbf{u}$), which are obviously correlated with the location of the crack. It is possible to show that the natural space for the setting of the variational problem is the space of Special functions of Bounded Variations SBV, so that $S[\mathbf{u}]$ is rectifiable (it is a set of curves in 2D). Therefore, meas($S[\mathbf{u}]$) denotes the (Hausdorff) measure $S[\mathbf{u}]$, which in 2D indicates the total length of the propagating cracks. Therefore, the significance of the second functional of Eq. (4.9) is that it establishes an energetic competition between the elastic strain energy stored in the solid, and the energy that is necessary to create new crack surfaces. It is then customary to think about phase-field models in the aforementioned limit. However, in the numerical applications one has to choose the quantity $\varepsilon\neq 0$ in order to avoid numerical instabilities. The values commonly used are of the order of $\varepsilon=0.01$, but this implies that the stiffness of the completely damaged material ($\phi=0$) is not null, but of the order of $\varepsilon(\lambda+2\mu)$. This provides a contribution that, in the limit of sharp cracks, is equivalent to the bridging of the crack lips by forces that are proportional to the COD. Such contribution cannot in general be neglected while calculating the energy release rate associated with the propagating crack.

4.2 The Generalized Eshelby Energy–Momentum Tensor.

In order to consider the additional dependence on the phase-field ϕ in the energy density function (4.1), it is necessary to introduce a GEM tensor that extends to phase-field models the Eshelby tensor [2]. Such a tensor, already proposed by Hakim and Karma [12], reads

$$\mathbf{T}_G = \Theta\,\mathbf{I} - \nabla\mathbf{u}^T\mathbf{S} - \nabla\phi\otimes\boldsymbol{\omega} \tag{4.10}$$

It is useful, for the following considerations, to report a direct verification of the fact that, if $\mathbf{T}_G$ is regular, for any closed path $\Gamma\subset\Omega$, the contour integral is null, i.e.,

$$J_G = \mathbf{r}\cdot\int_\Gamma \mathbf{T}_G\mathbf{n} = 0 \tag{4.11}$$

where $\mathbf{r}$ is any constant vector, and $\mathbf{n}$ is the outward unit normal to Γ. In fact, if B denotes the sub-body enclosed by Γ, recalling Eq. (4.5) one has

$$\begin{aligned} &\int_\Gamma \Theta\,\mathbf{r}\cdot\mathbf{n}\,ds\\ &= \int_B \nabla\Theta\cdot\mathbf{r}\,d\mathbf{x}\\ &= \int_B\left\{\frac{\partial\Theta}{\partial\nabla^s\mathbf{u}}\cdot(\nabla(\nabla^s\mathbf{u})\mathbf{r}) + \frac{\partial\Theta}{\partial\nabla\phi}\cdot(\nabla(\nabla\phi)\mathbf{r}) + \frac{\partial\Theta}{\partial\phi}\nabla\phi\cdot\mathbf{r}\right\}d\mathbf{x}\\ &= \int_B\left\{\mathbf{S}\cdot(\nabla(\nabla\mathbf{u})\mathbf{r}) + \boldsymbol{\omega}\cdot(\nabla(\nabla\phi)\mathbf{r}) + \frac{\partial\Theta}{\partial\phi}\nabla\phi\cdot\mathbf{r}\right\}d\mathbf{x} \end{aligned} \tag{4.12}$$

Moreover, integrating by parts and recalling Eq. (4.7), the result is

$$\begin{aligned}\mathbf{r}\cdot\int_\Gamma \Theta\,\mathbf{n}\,ds &= \int_\Gamma \left\{\mathbf{S}^T\nabla\mathbf{u}\,\mathbf{r}+(\nabla\phi\cdot\mathbf{r})\boldsymbol{\omega}\right\}\cdot\mathbf{n}ds\\ &\quad-\int_B\left\{\mathrm{Div}\,\mathbf{S}\cdot(\nabla\mathbf{u}\,\mathbf{r})+\left(\mathrm{Div}\,\boldsymbol{\omega}-\frac{\partial\Theta}{\partial\phi}\right)(\nabla\phi\cdot\mathbf{r})\right\}d\mathbf{x}\\ &=\int_\Gamma\left\{\mathbf{S}\mathbf{n}\cdot\nabla\mathbf{u}\,\mathbf{r}+(\nabla\phi\cdot\mathbf{r})\boldsymbol{\omega}\right\}\cdot\mathbf{n}ds\\ &=\mathbf{r}\cdot\int_\Gamma\left\{\nabla\mathbf{u}^T\mathbf{S}+(\nabla\phi\otimes\boldsymbol{\omega})\right\}\mathbf{n}ds\end{aligned}\tag{4.13}$$

from which Eq. (4.11) directly follows. Observe that a key hypothesis for the derivation of Eq. (4.11) is that no singularities, either in the strain or in the phase-field, are present inside the material. This hypothesis is verified in practice, because the material adapts to any possible stress concentrator by a variation of its stiffness, controlled by the phase field. Obviously, the generalized Eshelby tensor reduces to the classical expression where the material is sound, because in this case $\phi=1$ and $\nabla\phi=0$.

4.3 An Illustrative Example. In order to illustrate the use of the GEM tensor, it is useful to refer to the problem of the long strip extended between two platens, already considered in Sec. 3.3. This configuration is once more schematically represented as in Fig. 4(*b*), the difference being that now there is no crack, but instead a band of a certain width representing the phase field. A region that represents the counterpart of the crack tip can only be approximately localized, and we will suppose that the origin of reference system is located within this region. Because of symmetry, the displacement field and the phase field will be symmetric with respect to the line $x_2=0$.

Consider again the path Γ represented by the dashed *closed* contour *ABCD* shown in Fig. 4(*b*). In this case, the distinction of the branch P^-P^+ on *AB* is not possible, because it is not possible to identify the surfaces of the crack. In fact, the field ϕ varies smoothly while passing from $x_2=-H$ to $x_2=+H$; there is no neat transition between $\phi=0$ and $\phi=1$. A rough technical solution, sometimes adopted, could consist of identifying the crack as the region in which $\phi\le\phi_0<1$, but there is a great ambiguity in the definition of the value ϕ_0.

Consider the minimization problem (4.6), in which the energy density (4.1) is defined by Eqs. (4.3) and (4.4). The boundary conditions in terms of the displacement $\mathbf{u}$ are the same of those considered in Sec. 3.3. Concerning the phase field, on the clamped borders we may equivalently consider either the natural boundary conditions of the variational problem (4.6), i.e., $\nabla\phi\cdot\mathbf{n}=0$, or the geometric conditions $\phi=1$, as explained in Ref. [26]. Let us consider an advancement of the crack in the direction of positive x_1, so that $\mathbf{r}=\mathbf{e}_1$ in Eq. (4.11). On the paths *AD* and *BC*, one has that $\mathbf{r}\cdot(\nabla\phi\otimes\boldsymbol{\omega})\mathbf{n}=\boldsymbol{\omega}\cdot\mathbf{n}\ \nabla\phi\cdot\mathbf{e}_1$, which is null in any case if one assumes for $\boldsymbol{\omega}$ the expression (4.5). Therefore, the contribution of the GEM on these paths is zero. Moreover, if the paths *AB* and *CD* are sufficiently far from the origin, not only $\mathbf{S}\mathbf{n}$ but also $\boldsymbol{\omega}\cdot\mathbf{n}$ is null, because the field ϕ is in practice independent of x_1, i.e., $\phi_{,1}=0$. Therefore, on such paths, the only nonzero contribution comes from the integration of the energy density Θ.

Consider first the path *AB*. One needs to calculate

$$\begin{aligned}\mathbf{e}_1\cdot\int_{AB}\mathbf{T}_G\mathbf{n} &= -\int_{-H}^{H}\Theta\left[\mathbf{u}(x_{1P},x_2),\phi(x_{1P},x_2)\right]dx_2\\ &=-\int_{-H}^{H}\left\{(g(\phi)+h(\phi))\frac{1}{2}(\lambda+2\mu)(u_{2,2})^2\right.\\ &\quad\left.+\frac{1}{2}\gamma l(\phi_{,2})^2+\frac{\gamma}{2l}(1-g(\phi))\right\}dx_2\end{aligned}\tag{4.14}$$

But this integral coincides with the energy *per* unit x_1-width of the body in a portion sufficiently far from the origin, where the dependence upon x_1 can be neglected. Since the solution corresponds to the minimizer of the variational problem (4.6), the fields that must be considered in the integral (4.14) coincide with those that minimize the integral itself. In other words, sufficiently far from the "crack-tip" the problem becomes one-dimensional.

The Euler–Lagrange equations associated with the minimization of Eq. (4.14) are

$$\begin{aligned}&\frac{\partial}{\partial x_2}\left[(g(\phi)+h(\phi))(\lambda+2\mu)u_{2,2}\right]=0\\ &-\gamma l\,\phi_{,22}+\left(g'(\phi)+h'(\phi)\right)\frac{1}{2}(\lambda+2\mu)(u_{2,2})^2-g'(\phi)\frac{\gamma}{2l}=0\end{aligned}\tag{4.15}$$

Clearly Eq. $(4.15)_1$ represents equilibrium in the x_2 direction, while Eq. $(4.15)_2$ is the balance of the phase field.

From Eq. $(4.15)_1$, one has that

$$u_{2,2}=\sqrt{\frac{\gamma/l}{\lambda+2\mu}}\frac{c}{g(\phi)+h(\phi)}\tag{4.16}$$

where c is a dimensionless constant. Inserting this result in Eq. $(4.15)_2$, one obtains

$$-\gamma l\,\phi_{,22}+\frac{\gamma}{2l}\left[c^2\frac{g'(\phi)+h'(\phi)}{(g(\phi)+h(\phi))^2}-g'(\phi)\right]=0\tag{4.17}$$

This expression can be conveniently rewritten in the form

$$-\gamma l\,\phi_{,22}-\frac{\gamma}{2l}\frac{\partial}{\partial\phi}(V(\phi))=0\,,\quad\text{with } V(\phi)=\frac{c^2}{g(\phi)+h(\phi)}+g(\phi)\tag{4.18}$$

As suggested for the 1D problems considered in Refs. [11] and [12], it is convenient to consider a mechanical analogy, in which x_2 plays the role of time, and ϕ represents the position of a fictitious particle. Therefore, Eq. (4.18) represents the motion of such particle in the potential $V(\phi)$. With this analogy, the solution corresponds to the motion of the particle that starts at time $x_2=-H$ from $\phi=1$, with a negative velocity $\phi_{,2}$, to reach a minimum $\phi=\phi_m$ at $x_2=0$, where the velocity vanishes. From this turning point, it follows the time reversed motion and the particle comes back to $\phi=1$ at $x_2=+H$. The possibility of integrating the equations of motion requires the conservation law

$$\frac{1}{2}\gamma l\left(\phi_{,2}\right)^2+\frac{\gamma}{2l}V(\phi)=\frac{\gamma}{2l}V(\phi_m)\tag{4.19}$$

Since the outward path $-H$ to 0 ($\phi=1$ to ϕ_m) is symmetrical with respect to the return path 0 to H (ϕ_m to $\phi=1$), it is sufficient to consider just one of the two paths and to multiply by two the corresponding result. Considering the return path 0 to H (ϕ_m to $\phi=1$), one has from Eq. (4.19) that

$$\phi_{,2}=\frac{1}{l}\sqrt{V(\phi_m)-V(\phi)}\quad\Rightarrow\quad dx_2=\frac{l}{\sqrt{V(\phi_m)-V(\phi)}}d\phi\tag{4.20}$$

Then, Eq. (4.14) becomes

$$\int_{-H}^{H}\Theta\left[\mathbf{u}(x_{1P},x_2),\phi(x_{1P},x_2)\right]dx_2=\gamma\int_{\phi_m}^{1}\frac{1+V(\phi_m)-2g(\phi)}{\sqrt{V(\phi_m)-V(\phi)}}d\phi\tag{4.21}$$

In order to solve the problem, one needs to calculate the constants ϕ_m and c. Recalling Eqs. (4.20) and (4.16), these can be found from conditions

$$2H = \int_{-H}^{H} dx_2 = 2\int_{\phi_m}^{1} \frac{l\,d\phi}{\sqrt{V(\phi_m) - V(\phi)}}$$
$$\Rightarrow \quad \frac{H}{l} = \int_{\phi_m}^{1} \frac{d\phi}{\sqrt{V(\phi_m) - V(\phi)}} \tag{4.22}$$

and

$$2\Delta = \int_{-H}^{H} u_{2,2}dx_2 = 2\int_{\phi_m}^{1} \frac{c\sqrt{\gamma/(l(\lambda+2\mu))}\,d\phi}{(g(\phi)+h(\phi))\sqrt{V(\phi_m) - V(\phi)}}$$
$$\Rightarrow \quad \Delta\sqrt{\frac{\lambda+2\mu}{\gamma/l}} = c\int_{\phi_m}^{1} \frac{1}{g(\phi)+h(\phi)} \frac{d\phi}{\sqrt{V(\phi_m) - V(\phi)}} \tag{4.23}$$

where 2Δ denotes the total elongation of the strip in the x_2 direction. It is important to distinguish in the expression (4.14) the part that is associated with the elastic strain of the material, say $E_{\mathrm{el},AB}$, from that that is expended in the modification of the phase field, referred to as $E_{\mathrm{pf},AB}$. One clearly has

$$E_{\mathrm{el},AB} = \int_{-H}^{H} (g(\phi)+h(\phi))\frac{1}{2}(\lambda+2\mu)(u_{2,2})^2 dx_2,$$
$$E_{\mathrm{pf},AB} = \int_{-H}^{H} \left\{\frac{1}{2}\gamma l(\phi_{,2})^2 + \frac{\gamma}{2l}(1-g(\phi))\right\} dx_2 \tag{4.24}$$

Using Eqs. (4.16) and (4.23), one finds

$$E_{\mathrm{el},AB} = 2\int_0^H \frac{\gamma}{2l}\frac{c^2}{g(\phi)+h(\phi)}dx_2$$
$$= \frac{\gamma}{l}c\int_{\phi_m}^{1} \frac{c}{g(\phi)+h(\phi)}\frac{d\phi}{\sqrt{V(\phi_m) - V(\phi)}} = c\Delta\sqrt{\frac{\gamma}{l}(\lambda+2\mu)} \tag{4.25}$$

On the other hand, from Eq. (4.16), one also finds that the stress component $\sigma_{22}(x_{1AB}, \pm H)$, in a neighborhood of $x_2 = \pm H$, where $\phi \cong 1$, takes the form

$$\sigma_{22}(x_{1AB}, \pm H) = \big(g(1)+h(1)\big)(\lambda+2\mu)u_{2,2}(x_{1AB}, \pm H)$$
$$= c\sqrt{\frac{\gamma}{l}(\lambda+2\mu)} \tag{4.26}$$

so that Eq. (4.25) reads

$$E_{\mathrm{el},AB} = \frac{1}{2}\sigma_{22}(x_{1AB}, \pm H)2\Delta \tag{4.27}$$

This is nothing but Clapeyron theorem for linear elastic materials. The evaluation of the second term of Eq. (4.24) is less straightforward, but can be readily obtained in the limit case $H/l \gg 1$. In the mechanical analogy with the motion of the particle, this means that the time H that is necessary to pass from $\phi = \phi_m$ to $\phi = 1$ tends to infinity. Therefore, following the same argument of Ref. [12], this means that in the energetic balance of Eq. (4.19) one has $V(\phi_m) = V(1) + O_\varepsilon$, where O_ε is an infinitesimal quantity. Recalling Eq. (4.19), this gives conditions

$$\frac{c^2}{g(\phi_m)+h(\phi_m)} + g(\phi_m) = \frac{c^2}{g(1)+h(1)} + 1 + O_\varepsilon \tag{4.28}$$

from which one finds

$$c^2 = \frac{(1-g(\phi_m)+O_\varepsilon)\big(g(1)+h(1)\big)\big(g(\phi_m)+h(\phi_m)\big)}{\big(g(1)+h(1)\big) - \big(g(\phi_m)+h(\phi_m)\big)} \tag{4.29}$$

Then, after substitution in Eq. (4.18), one obtains

$$V(\phi_m) - V(\phi) = 1 - g(\phi) + O_\varepsilon + q(\phi, \phi_m)$$
$$\text{with } q(\phi, \phi_m)$$
$$= \frac{(1-g(\phi_m)+O_\varepsilon)\big(g(\phi_m)+h(\phi_m)\big)\big(g(\phi)+h(\phi)-g(1)-h(1)\big)}{\big(g(1)+h(1)\big) - \big(g(\phi_m)+h(\phi_m)\big)} \tag{4.30}$$

Using the expressions (4.4) for $g(\cdot)$ and $h(\cdot)$, and recalling that $\phi_m \ll 1$, one finds, up to first order in ϕ_m, that

$$q(\phi, \phi_m) = \frac{(1-\phi_m(2-\phi_m)+O_\varepsilon)\left(\phi_m^2+\varepsilon\right)\left(\phi^2-1\right)}{1-\phi_m^2}$$
$$\cong \left(\phi_m^2+\varepsilon\right)\left(\phi^2-1\right) \tag{4.31}$$

and

$$c^2 = \frac{(1-\phi_m(2-\phi_m)+O_\varepsilon)(1+\varepsilon)\left(\phi_m^2+\varepsilon\right)}{1-\phi_m^2} \cong \left(\phi_m^2+\varepsilon\right) \tag{4.32}$$

where "$\cong$" means "up to higher order terms in ϕ_m." If in the expression (4.30), the quantity $q(\phi, \phi_m)$ is neglected together with O_ε with respect to the other, one simply obtains that

$$V(\phi_m) - V(\phi) \cong 1 - g(\phi) = (1-\phi)^2 \tag{4.33}$$

Consequently, substituting in Eq. (4.24), taking into account Eqs. (4.19) and (4.20), one finally obtains

$$E_{\mathrm{pf},AB} = 2\int_{\phi_m}^{1} \frac{\gamma}{2l}\frac{V(\phi_m) - V(\phi) + 1 - g(\phi)}{\sqrt{V(\phi_m) - V(\phi)}} l\,d\phi$$
$$\cong 2\gamma\int_{\phi_m}^{1} \sqrt{1-g(\phi)}d\phi = 2\gamma\int_{\phi_m}^{1} (1-\phi)d\phi = \gamma \tag{4.34}$$

If the term $q(\phi, \phi_m)$ in Eq. (4.30) is not neglected, the calculations become more complicated. The term $E_{\mathrm{pf},AB}$ would result in general different from γ, but it could be calculated with a simple numerical approach. In order to complete the evaluation of the contour integral J_G of Eq. (4.11), one needs to evaluate the value on the path CD. Here, the calculation is straightforward because here $\phi = 1$ and, consequently, $u_{2,2}(x_{1CD}, x_2) = \text{cost} = \Delta/H$. Therefore

$$\mathbf{e}_1 \cdot \int_{CD} \mathbf{T}_G\mathbf{n} = \int_{-H}^{H} \frac{1}{2}(\lambda+2\mu+\varepsilon)(u_{2,2})^2 dx_2$$
$$= \frac{1}{2}(\lambda+2\mu+\varepsilon)\frac{\Delta^2}{H^2}2H = (\lambda+2\mu+\varepsilon)\frac{\Delta^2}{H} \tag{4.35}$$

In conclusion, using the previous results, one obtains

$$0 = J_G \cong -\sigma(x_{1AB}, \pm H)\Delta - \gamma + (\lambda+2\mu+\varepsilon)\Delta^2/H \tag{4.36}$$

from which it is possible to calculate $\sigma(x_{1AB}, \pm H)$ and, from Eq. (4.26), the constant c.

The displacement $u_2(x_{1AB},x_2)$ can be obtained as the parametric plot of $[x_2(\phi),\ u_2(\phi)]$, for ϕ varying in the range $\phi \in [\phi_m,1]$, through the relationships

$$x_2(\phi) = \int_0^{x_2(\phi)} dx_2 = \int_{\phi_m}^{\phi} \frac{l\,d\phi}{\sqrt{V(\phi_m) - V(\phi)}}\,,$$
$$u_2(\phi) = \int_0^{x_2(\phi)} u_{2,2} dx_2 = \int_{\phi_m}^{\phi} \frac{c\sqrt{\gamma l/(\lambda + 2\mu)}\ d\phi}{(g(\phi) + h(\phi))\sqrt{V(\phi_m) - V(\phi)}} \tag{4.37}$$

In these expressions, all the parameters are known once the values of c and ϕ_m have been determined.

4.4 The Energy Release Rate of a Phase-Field Crack and the Effective GEM (EGEM) Tensor. In order to correlate the phase-field approach with classical LEFM, it is important to define what in terms of LEFM is the energy release rate. One could consider an argument similar to the one that, for the case of bridged cracks, has brought to the definition of the effective strain energy Ψ^* and of the J^* integral of Eq. (3.18).

For the case of phase-field cracks, differently from Eq. (4.10), the EGEM tensor can be defined as

$$\mathbf{T}_G^* = \Theta^* \mathbf{I} - \nabla \mathbf{u}^T \mathbf{S} - \nabla\phi \otimes \boldsymbol{\omega}\,, \quad \Theta^* = \Theta - \Theta_{\text{pf}} \tag{4.38}$$

where Θ_{pf} is the part of the energy density that is associated with the intrinsic dissipation from the phase field. To illustrate, assuming an energy density of the type of Eq. (4.1), one has that

$$\Theta^* = \Theta^*[\mathbf{u},\phi] = (g(\phi) + h(\phi))\frac{1}{2}\mathbf{C}\nabla^s\mathbf{u} \cdot \nabla^s\mathbf{u}\,,$$
$$\Theta_{\text{pf}} = \Theta_{\text{pf}}[\phi] = w(\nabla\phi) + (1 - g(\phi))\frac{\gamma}{2l} \tag{4.39}$$

Reasoning as in Eqs. (4.12) and (4.13), it can be proved that

$$J_G^* = \mathbf{r} \cdot \int_\Gamma \mathbf{T}_G^* \mathbf{n} = \mathbf{r} \cdot \int_\Gamma \mathbf{T}_G \mathbf{n} - \mathbf{r} \cdot \int_\Gamma \Theta_{\text{pf}} \mathbf{n} = -\mathbf{r} \cdot \int_\Gamma \Theta_{\text{pf}} \mathbf{n} \tag{4.40}$$

Therefore, if one considers a path Γ that traverses the band of damaged material, and if $\mathbf{r}$ denotes the direction of the propagating band, then the integral involving Θ_{pf} can capture a quantity that is associated with the rate of energy dissipated during the propagation process. In the energetic balance *à la* Griffith, such quantity can be associated with the elastic energy release rate. The conclusion is therefore that

$$\text{energy release rate} = -J_G^* = -\mathbf{r} \cdot \int_\Gamma \mathbf{T}_G^* \mathbf{n}$$
$$= -\mathbf{r} \cdot \int_\Gamma (\Theta^* \mathbf{I} - \nabla^s \mathbf{u}^T \mathbf{S} - \nabla\phi \otimes \boldsymbol{\omega})\mathbf{n} \tag{4.41}$$

where Γ is any path traversing the damaged band. Of course, one should make sure that indeed the path traverses the whole band and passes through regions that are not affected by the propagation of the band. For example, if a path of the type $P^-P^+S^+C\,S^-P^-$ is considered, one should choose it sufficiently far from the band tip, so that $\phi \cong 1$ at points P^-, P^+, S^+, S^-, and on the circle C. If this is not the case, when the crack advances the integral J_G^* would capture *only* the rate of dissipation of the energy associated with the transformations occurring in the region comprised *inside* the path Γ. In other words, if the movement of the band produces a variation of the phase field also in material portions that are not enclosed by Γ, this contribution would be lost while evaluating J_G^*.

Finally, note that there is a strict correlation between the J^* integral defined in Eq. (3.18), which refers to bridged cracks, and the integral J_G^* of Eq. (4.40), associated with phase-field cracks. The correlation is provided by the Γ-convergence result (4.9) for the case in which the model is of the type considered in Ref. [13]. In fact, since in the limit $l \to 0$, the phase-field model converges (more precisely Γ-converges) to the sharp crack model, in this case the integral J_G^* of Eq. (4.40) would tend to J^* of Eq. (3.18).

5 Conclusions

An alternative application has been proposed for the use of the J-integral to calculate the energy release rate of a moving crack. The main difference with respect to the classical method, originally developed by Rice, consists in considering closed paths that traverse the crack discontinuity, picking up in the branch comprised by the crack gap various possible sources of dissipation. By means of paradigmatic examples, it has been shown that the closed-path J-integral method can be readily applied to bridged crack models (nonvanishing crack tip stress intensity factor) as well as to traditional cohesive zone models (vanishing stress intensity factor) providing, in the small-scale bridging limit, the classical energetic balance *à la* Griffith. In fact, this extended form of the J-integral results to be null on every closed path, a finding that is equivalent to state that the energy release rate on the moving crack must equal the energy dissipated to break the material ligaments. A proper definition of the energy momentum tensor allows us to sort out the two aforementioned contributions and to calculate the energy release rate. The method provides a parallelism with the use of Eshelby's energy–momentum tensor on dislocations, whose flux is calculated on closed path embracing the source of imperfection.

It was also demonstrated that the proposed method can be useful in the formulations of phase-field models of crack propagation, where there is no material discontinuity and sharp cracks are substituted by thin bands where damage accumulates. The use of the closed-path approach eliminates the need to identify precisely the boundary of the propagating band, as instead required in the approach proposed by other authors. Moreover, appropriately introducing an enhanced form of GEM tensor for phase-field models, it is possible to calculate, with the contour integral, the energy release rate associated with a propagating band. With some modification, the method could certainly be applied also when other phenomena of interaction occur at the crack surfaces, an example of which could be represented by the effects of the electric fields and chemical transformations.

The results shown in this article have been verified through a direct calculation in the near-tip region approximation of a straight semi-infinite crack (or damage band), quasi-statically and monotonically propagating in an infinite medium. Recent works have proved that the use of Eshelby's energy momentum tensor and the J-integral has a wide applicability, because it can be applied to a class of materials much broader than only superelastic materials, i.e., materials for which the stress can be uniquely derived from a potential. However, a more general proof of the applicability of the closed-path approach on dissipative interfaces, including time-dependent situation, is still required. Dissipative media indeed present difficulties since the governing equation is not self-adjoint. In the cases considered in this article, the difficulty is by-passed, because only monotone loading histories and smoothly propagating cracks (or damage bands) are considered. Certainly, loading–unloading conditions should be regarded with great care, and the correct application of the closed-path J-integral is yet to be established, especially when dynamic aspects are of importance. Further attention should also be paid at more complex crack geometries, other than the straight crack configuration analyzed here.

In summary, the proposed application of the J-integral on closed paths appears promising, because it is very general, it applies to both sharp cracks and damage bands, and it can in

general take into account the most various forms of damaging interaction between material particles. The proposed method opens the possibility of including the effects of chemical processes and electromagnetic fields.

Acknowledgment

The authors thank Dr. Chad Landis for useful discussions related to the closed contour *J*-integral approach for phase-field cracks and for providing us some of his classroom notes that include derivations that parallel those presented in Sec. 4 of this paper. R.B. acknowledges the Thomas and Laura Hsu Professorship and the National Science Foundation under Grant No. CMMI-1361868. G.R.C. acknowledges the support of the European Community under Contract No. RFSR-CT-2012-00026 (S+G RFS-PR-11017).

References

[1] Eshelby, J. D., 1951, "The Force on Elastic Singularity," Philos. Trans. R. Soc. London, Ser. A, **244**(877), pp. 87–112.
[2] Eshelby, J., 1975, "The Elastic Energy-Momentum Tensor," J. Elasticity, **5**(3–4), pp. 321–335.
[3] Gurtin, M., 1995, "The Nature of Configurational Forces," Arch. Ration. Mech. Anal., **131**(1), pp. 67–100.
[4] Gurtin, M., 2008, *Configurational Forces as Basic Concepts of Continuum Physics*, Springer Science & Business Media, New York.
[5] Gurtin, M., and Podio-Guidugli, P., 1996, "Configurational Forces and the Basic Laws of Crack Propagation," J. Mech. Phys. Solids, **44**(6), pp. 905–927.
[6] Rice, J. R., 1968, "A Path Independent Integral and the Approximate Analysis of Strain Concentration by Notches and Cracks," ASME J. Appl. Mech., **35**(2), pp. 379–386.
[7] Fosdick, R., and Royer-Carfagni, G., 2005, "A Stokes Theorem for Second-Order Tensor Fields and Its Implications in Continuum Mechanics," Int. J. Non-Linear Mech., **40**(2–3), pp. 381–386.
[8] Love, A., 1927, *A Treatise on the Mathematical Theory of Elasticity*, 4th ed., Cambridge University Press, Cambridge.
[9] Barenblatt, G. I., 1962, "The Mathematical Theory of Equilibrium Cracks in Brittle Fracture," Adv. Appl. Mech., **7**, pp. 55–129.
[10] da Silva, M., Duda, F., and Fried, E., 2013, "Sharp-Crack Limit of a Phase-Field Model for Brittle Fracture," J. Mech. Phys. Solids, **61**(11), pp. 2178–2195.
[11] Karma, A., Kessler, D., and Levine, H., 2001, "Phase-Field Model of Mode III Dynamic Fracture," Phys. Rev. Lett., **87**(4), p. 455011.
[12] Hakim, V., and Karma, A., 2009, "Laws of Crack Motion and Phase-Field Models of Fracture," J. Mech. Phys. Solids, **57**(2), pp. 342–368.
[13] Bourdin, B., Francfort, G., and Marigo, J. J., 2000, "Numerical Experiments in Revisited Brittle Fracture," J. Mech. Phys. Solids, **48**(4), pp. 797–826.
[14] Ambrosio, L., and Tortorelli, V., 1990, "Approximation of Functionals Depending on Jumps by Elliptic Functionals Via Gamma-Convergence," Commun. Pure Appl. Math., **43**(8), pp. 999–1036.
[15] Frémond, M., and Nedjar, B., 1996, "Damage, Gradient of Damage and Principle of Virtual Power," Int. J. Solids Struct., **33**(8), pp. 1083–1103.
[16] Francfort, G., and Marigo, J., 1998, "Revisiting Brittle Fracture as an Energy Minimization Problem," J. Mech. Phys. Solids, **46**(8), pp. 1319–1342.
[17] Sarrado, C., Turon, A., Costa, J., and Jordi, R., 2016, "On the Validity of Linear Elastic Fracture Mechanics Methods to Measure the Fracture Toughness of Adhesive Joints," Int. J. Solids Struct., **81**, pp. 110–116.
[18] Bhandakkar, T., and Gao, H., 2011, "Cohesive Modelling of Crack Nucleation in a Cylindrical Electrod Under Axisymmetric Diffusion Induced Stresses," Int. J. Solids Struct., **48**(16–17), pp. 2304–2309.
[19] Gao, H., Zhang, T.-Y., and Tong, P., 1997, "Local and Global Energy Release Rates for an Electrically Yielded Crack in a Piezoelectric Ceramic," J. Mech. Phys. Solids, **45**(4), pp. 491–510.
[20] Goutianos, S., and Sorensen, B. F., 2016, "The Application of J-Integral to Measure Cohesive Laws Under Large-Scale Yielding," Eng. Fracture Mech., **155**, pp. 145–165.
[21] Cox, B., and Marshall, D. B., 1994, "Concepts for Bridged Cracks in Fracture and Fatigue," Acta Metall. Mater., **42**(2), pp. 341–363.
[22] Aveston, J., and Kelly, A., 1973, "Theory of Multiple Fracture of Fibre Composites," J. Mater. Sci., **8**(3), pp. 352–362.
[23] Willis, J., 1967, "A Comparison of the Fracture Criteria of Griffith and Barenblatt," J. Mech. Phys. Solids, **15**(3), pp. 151–162.
[24] Freddi, F., and Royer-Carfagni, G., 2010, "Regularized Variational Theories of Fracture: A Unified Approach," J. Mech. Phys. Solids, **58**(8), pp. 1154–1174.
[25] Focardi, M., 2001, "On the Variational Approximation of Free-Discontinuity Problems in the Vectorial Case," Math. Models Methods Appl. Sci., **11**(04), pp. 663–684.
[26] Lancioni, G., and Royer-Carfagni, G., 2009, "The Variational Approach to Fracture Mechanics. A Practical Application to the French Panthéon in Paris," J. Elasticity, **95**(1), pp. 1–30.